Mobility of crocidolite asbestos in sandy porous media mimicking aquifer systems

Journal of Hazardous Materials 458 (2023) 131998

Contents lists available at ScienceDirect

Journal of Hazardous Materials

journal homepage: www.elsevier.com/locate/jhazmat

Mobility of crocidolite asbestos in sandy porous media mimicking aquifer systems

Leonardo Magherini [a], Chiara Avataneo [b,c], Silvana Capella [b,c], Manuela Lasagna [b], Carlo Bianco [a], Elena Belluso [b,c,d], Domenico Antonio De Luca [b], Rajandrea Sethi [a,e,*]

[a] Department of Environment, Land and Infrastructure Engineering (DIATI), Politecnico di Torino, Corso Duca degli Abruzzi 24, 10129 Turin, Italy
[b] Department of Earth Sciences, University of Turin, Via Valperga Caluso 35, 10125 Turin, Italy
[c] "G. Scansetti" Interdepartmental Center for Studies on Asbestos and Other Toxic Particulates, University of Turin, Via Pietro Giuria 7, 10125 Turin, Italy
[d] Geosciences and Earth Resources (IGG) of the National Research Council of Italy (CNR), Operational Unit of Turin, Via Valperga Caluso 35, 10125 Turin, Italy
[e] Clean Water Center (CWC), Politecnico di Torino, Corso Duca degli Abruzzi 24, 10129 Turin, Italy

HIGHLIGHTS

- 5-to-10-μm-long crocidolite is transported through sandy porous media.
- Crocidolite longer than 10 μm is mobile in coarse sand aquifers.
- A geochemical modification of groundwater can mobilise crocidolite.
- Groundwater is a potential migration/exposure pathway for asbestos.

GRAPHICAL ABSTRACT

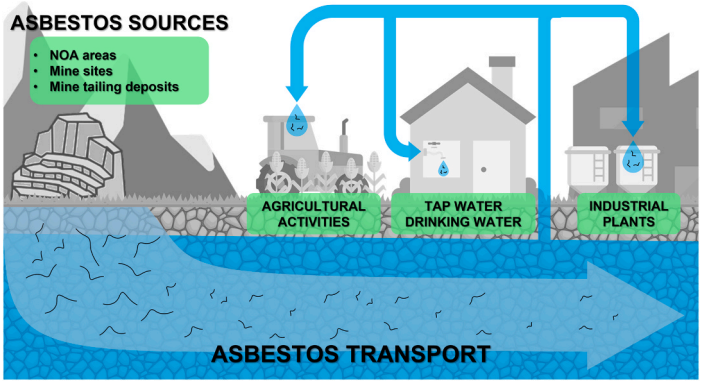

ARTICLE INFO

Editor: John D. Atkinson

Keywords:
Asbestos transport
Fibre mobility
Crocidolite
Groundwater
Column test

ABSTRACT

Asbestos is widely recognized as being a carcinogen when dispersed in air, but very little is known about its exposure pathways in water and its subsequent effects on human health. Several studies have proved asbestos presence in groundwater but failed to assess its mobility in aquifer systems. This paper aims to fill this gap by studying the transport of crocidolite, an amphibole asbestos, through sandy porous media mimicking different aquifer systems. To this purpose, two sets of column test were performed varying the crocidolite suspension concentration, the quartz sand grain size distribution, and the physicochemical water parameters (i.e., pH). The results proved that crocidolite is mobile in quartz sand due to the repulsive interactions between fibres and porous media. The concentration of fibres at the outlet of the column were found to decrease when decreasing the grain size distribution of the porous medium, with a bigger impact on highly concentrated suspensions. In particular, 5-to-10-μm-long fibres were able to flow through all the tested sands while fibres longer than 10 μm

* Corresponding author at: Department of Environment, Land and Infrastructure Engineering (DIATI), Politecnico di Torino, Corso Duca degli Abruzzi 24, 10129 Turin, Italy.
E-mail address: rajandrea.sethi@polito.it (R. Sethi).

https://doi.org/10.1016/j.jhazmat.2023.131998
Received 27 March 2023; Received in revised form 19 June 2023; Accepted 3 July 2023
Available online 4 July 2023

were mobile only through the coarser medium. These results confirm that groundwater migration should be considered a potential exposure pathway while implementing human health risk assessment.

1. Introduction

Asbestos is the commercial term that indicates a group of six naturally occurring silicate minerals with fibrous morphology. This group includes one serpentine phyllosilicate (chrysotile) and five amphiboles, which are chain silicates (tremolite asbestos, actinolite asbestos, anthophyllite asbestos, amosite, and crocidolite). In the past, these minerals have been widely employed for industrial applications due to their valuable technological properties, such as resistance to heat, fire, chemical and biological degradation. Nowadays their application has been drastically decreased, or even banned by several countries [20], due to their adverse effects on human health. Indeed, the International Agency for Research on Cancer classifies asbestos as carcinogenic of the first group [19] and it is widely recognized as an air pollutant. For this reason, the European Union (EU) established an air concentration limit in the workplace for respirable fibres, i.e. fibres with length > 5 μm, width < 3 μm and aspect ratio (AR, length to width) > 3 [50], which are the ones considered to have carcinogenic effects when respired. The limit is 100 fibres per litre (f/L) [11] and is applied to the average air concentration measured during an 8 h work shift. The same limit is also applied in the United States by the U.S. Occupational Safety and Health Administration [32].

In the last decades, the attention of researchers and regulators shifted from occupational to environmental exposure scenarios. In particular, asbestos can be released by the erosion of Naturally Occurring Asbestos (NOA) or by mining and industrial activities (e.g. [28,37]). An outdoor attention threshold of 1 f/L for ambient air was therefore proposed by the EU in the air quality guidelines to regulate asbestos exposure in non-occupational environments [49].

Up until recently, legislations on asbestos have however only focused on regulating its presence in air, neglecting to consider migration pathways and subsequent human exposure via water. This is partially due to the fact that the effects of waterborne asbestos ingestion on human health are still unclear and have only recently begun to be studied by the scientific community [10,14,27]. As a consequence, carcinogenicity related to ingestion has not been scientifically proven up to date [48].

Nevertheless, the current literature identifies two main human exposure pathways for waterborne asbestos: (i) direct ingestion of asbestos containing water or beverages [9]; (ii) respiration of nebulised contaminated water droplets (e.g. [4,38]) or of resuspended fibres after polluted water vaporisation/evaporation. For the first scenario, the U.S. Environmental Protection Agency (US-EPA) established a maximum contaminant level in drinking water of $7{\cdot}10^6$ f/L for fibres longer than 10 μm [44] as a precautionary measure based on in vivo studies [30]. Instead, the legislation regarding airborne asbestos and its limits could be applied to the second scenario, but it has been traditionally neglected, even if it can determine a significant respiration exposure.

Besides drinking water, also freshwater resources should be monitored, in particular groundwater, which is one of the main sources of water for human consumption and anthropogenic activities. Indeed, groundwater is at the basis of many agricultural and industrial activities, as well as drinking water supply plants (e.g. [24]). The presence of asbestos in groundwater has been documented by several studies, which found fibres in aquifers that are naturally rich in asbestos [17,3,31,47] or in areas where the mobilization of the fibres is further enhanced by human activities, e.g. in the proximity of mines and mine tailing deposits [22,43,7]. More specifically, three studies have investigated asbestos occurrence in groundwater close to the former chrysotile mine of Balangero, Italy [3,43,7]. Based on analyses by Scanning Electron Microscopy coupled with Energy Dispersive Spectroscopy (SEM-EDS), Buzio et al. (2000) [7] detected an asbestos content of 1.00 mg/L to 4.10 mg/L in groundwater and reported that the presence of fibres was reduced by a factor 10 at a distance of 5 km from the mine discharge. Similarly, Turci et al. (2016) [43] monitored two wells in proximity of the former mine and detected over 10^6 f/L in the sampling point close to the mine southern tailings. Avataneo et al. (2021) [3] instead reported a variable asbestos content in wells or piezometers located in the alluvial plain close to the former asbestos mine of Balangero. Based on Transmission Electron Microscopy (TEM)-EDS, fibres up to 13 μm long were found in a sampling point with a concentration of $6.7{\cdot}10^6$ f/L (corresponding to 2 μg/L). Conversely, a study conducted on three drainage pits located next to a Russian asbestos deposit showed a very low asbestos concentration detected by means of Phase Contrast Optical Microscopy. The maximum concentration was $0.99{\cdot}10^5$ f/L with fibres longer than 5 μm ranging between 9.82% and 44.58% of the total [22]. Studies conducted in the U.S. in the '70 and '80 on samples collected from wells and springs and analysed by TEM-EDS showed the occurrence of asbestos in groundwater, mainly caused by the leaching of asbestos from the host rock formations. In particular, asbestos concentrations in the range $2{\cdot}10^7$-$2{\cdot}10^8$ f/L were found in California [17], while values over $2{\cdot}10^9$ f/L (0.91 μg/L) were found along the Rio Grande Valley, New Mexico [31]. In the Dayao region, China, a thin layer of outcrop crocidolite ore is spread on an area of around 200 km^2, resulting in an average groundwater asbestos contamination of $8.6{\cdot}10^6$ f/L, detected by SEM-EDS analyses [47].

Furthermore, the breaking and leaching of asbestos cement pipes - which have been extensively installed in the past in Europe and North America and are still used for drinking water distribution network - due to different factors, such as water quality, soil type, and climate (e.g., [1,18]), might constitute another asbestos environmental dispersion mechanism. This asbestos source, yet poorly studied, could cause soil and groundwater pollution, as well as drinking water contamination itself.

The above-mentioned studies only focused on the presence of asbestos in groundwater, failing to consider the mobility and transport of fibres through the aquifer systems. Indeed, the mobility of asbestos in the subsurface has always been neglected or considered irrelevant in the literature [21,33,46]. The contamination scenarios mentioned in previous studies can therefore imply relevant environmental and sanitary issues, especially if asbestos is able to migrate through porous media such as aquifer systems. An accurate study of asbestos mobility and transport is therefore needed to implement and integrate the knowledge of previous work to provide a comprehensive assessment of the health risks connected to migration via groundwater.

The well-established knowledge on particle transport in aquifer systems can be adapted to the case of asbestos. The colloidal transport in porous media is governed by advection, dispersion and by physical and physicochemical interactions with solid phase. Physical factors include the size and shape of the particles [34,39,41], the characteristics of the porous medium and the flow conditions [6]. Thanks to their typical form factor (length >> width), fibres can flow through pores that are smaller than their length but bigger than their width. On the other side, the elongation of the particles associated with drag forces can lead to filtration due to mechanical and geometrical interactions with the porous medium [39]. These interactions are further increased by aggregation and tangling [8,51]. Water chemistry, especially ionic strength and pH, can strongly influence the transport of particles by modifying the intensity of the attractive/repulsive forces acting between the fibres and the porous medium [16,36,40,5].

The transport of particles is also affected by the electrostatic interactions between the particles and the porous media. Chrysotile, at

neutral pH, is retained within the aquifer system due to the attractive electrostatic interaction between the positive surface charge of the fibres [35] and the net negative surface charge of the soil [15]. A recent study confirmed that bare chrysotile is not mobile in porous media but that, in presence of dissolved organic matter (DOM), its surface charge can be reverted thus allowing the subsurface transport [29]. As opposed to serpentine phyllosilicate, amphiboles naturally exhibit a negative net surface charge in water at any pH [35]. For this reason, these minerals are expected to be mobile in subsurface environments, due to the repulsive electrostatic interaction between the fibre and the negative surface of the porous medium.

The goal of this study is to verify if amphibole fibres, i.e. a naturally negatively charged asbestos, can be transported through saturated sandy aquifer systems without any surface modifier (or DOM). To this purpose, laboratory transport tests in sand-packed columns were performed using crocidolite as a representative amphibole asbestos. The tests were performed by varying the crocidolite concentration, the sand grain size distribution and the porewater composition with the aim to investigate: (i) to what extent crocidolite can be mobile in sandy porous media; (ii) how the size of fibres and pores affect the crocidolite mobility; (iii) if the groundwater physicochemical parameters influence the fibre transport.

2. Materials and methods

2.1. Asbestos suspensions

An asbestos suspension was prepared by adding crocidolite UICC (Union for International Cancer Control), a well characterised standard [23], to deionized water to obtain a 300 mg/L concentration. The crocidolite was dispersed in water applying sonication and stirring for about 25 min. The crocidolite suspension was characterised by a pH of 7.7 and a zeta potential of -30.2 ± 0.4 mV in 0.01 M NaCl, measured by dynamic light scattering (DLS Zetasizer Nano Z, Malvern Instruments Ltd., U.K.). A 1 mM MOPS buffer (MOPS, 3-N-Morpholino propanesulfonic acid, Sigma-Aldrich) was added to stabilise the pH at 6–7.

Two batches were prepared:

- a high concentration suspension (hereafter referred to as HC) obtained by collecting the supernatant of the 300 mg/L crocidolite suspension after 5 h settling (time required for settling of the largest fibres and achievement of a substantially stable suspension);
- a low concentration suspension (hereafter referred to as LC) obtained by filtering the HC suspension through a 11 cm coarse sand bed.

The batches were used to simulate two different scenarios: the asbestos transport near a concentrated contamination source using the HC batch, and the fibre fate at medium to long distance from the source thus using LC batch.

2.2. Porous media

Transport experiments were conducted in quartz sand (Dorsilit from Dorfner GmbH & Co., Germany). Three types of sand with different grain size distributions (Fig. S1, Supplementary Information-SI), defined respectively coarse, medium, and fine, were tested. The measured values of d_{10}-d_{50}-d_{90} were 1.31–1.59–1.91 mm for coarse sand, 0.48–0.68–0.84 mm for medium sand and 0.26–0.49–0.58 mm for fine sand. Before use, the sand was thoroughly cleaned to remove any residual impurities and colloids. The cleaning procedure consisted of three cycles of washing and sonication with 100 mM NaOH, tap water and deionized water, respectively. After cleaning, the sand was dried with a laboratory hot plate. Prior to packing the columns, a known quantity of dry sand was rehydrated in a 1 mM MOPS solution and degassed with a vacuum bell.

The zeta potential of each porous medium was measured in 0.01 M NaCl solution by DLS (Zetasizer Nano ZS90, Malvern Instruments Ltd., U.K.) after the sand was crushed dry with a ceramic mortar. The zeta potential was equal to -46.8 ± 1.0 mV, -49.1 ± 2.6 mV and -52.5 ± 0.6 mV, respectively for coarse, medium and fine sand.

The hydrodynamic parameters of the porous media, namely effective porosity and dispersivity, were determined by fitting a breakthrough curve (BC) of a conservative tracer (i.e. 10 mM NaCl in 1 mM MOPS). The estimated effective porosity was 47%, 43% and 39% for coarse, medium and fine sand, respectively. While the dispersivity was 0.47 mm for the coarse sand, 0.20 mm for the medium sand and 0.10 mm for the fine sand. The BCs and the parameters are reported in Fig. S2 and Table S1 of SI, respectively.

2.3. Column test setup, sampling, and injection procedure

The experimental setup is outlined in Fig. 1. A column with internal diameter of 1.6 cm and total length of 11 cm was vertically wet packed as follows: coarse sand was used to create a 0.5 cm drain at the column inlet and outlet; coarse, medium or fine sand, depending on the specific experiment conditions, were used to pack the 10 cm porous medium to be tested. After the column was vertically wet packed, it was set horizontally for the column test to mimic the horizontal flow in an aquifer system. The outlet tube was placed higher than the column to guarantee the saturation during the entire duration of the test.

The crocidolite suspension, continuously stirred, was pumped into the saturated column with a peristaltic pump at a flow rate of 0.22 ± 0.01 mL/min, corresponding to a Darcy velocity of 1.56 ± 0.09 m/d. The injection schedule was applied for all the tests as described below.

(i) Preconditioning: 10 pore volumes (PV) of a 1 mM MOPS solution to equilibrate the sand column.
(ii) Injection: 6 PV of crocidolite suspension (HC or LC) to test the asbestos transport.
(iii) Flushing: 3 PV of a 1 mM MOPS solution to flush the system.
(iv) Release: 3 PV of a solution containing 1 mM MOPS and 100 mM NaOH (pH 13) to induce the detachment of the total fraction of fibres that were reversibly deposited on the porous media during phase (ii).

During the experiments, the concentration of crocidolite suspension at the column outlet was measured online, via optical density measurements using a UV–vis spectrophotometer (Specord S600, Analytik Jena, Germany) equipped with a flow-through cell (Hellma, Germany). A linear relation between absorbance and crocidolite concentration was found at a wavelength of 285 nm (Fig. S3-S4-S5, SI). Throughout the paper "C" will be used to refer to the absorbance of crocidolite concentration measured by the spectrophotometer for outlet liquid samples, whereas "C_0" to refer to the absorbance concentration at the inlet.

During the column tests "L" liquid samples (Fig. 1) were collected at the column outlet every 1 PV. At the end of each test, the column was dissected and porous medium "S" samples (Fig. 1) of the first centimetre of porous medium were collected to examine the morphology of the fibres filtered out by the column. Both "L" and "S" sample types were then analysed by means of SEM-EDS.

2.4. SEM-EDS analyses

Both liquid "L" and solid "S" samples were collected during each column test and analysed by means of SEM-EDS, adapting the method proposed by the Regional Agency for the Protection of the Environment of Piedmont (Italy) [2] where this study was carried out. An aliquot (dependent on suspension turbidity) of the liquid samples was first filtered on a polycarbonate membrane (25 mm diameter, 0.1 μm porosity) using a vacuum filtration system. To prevent the sedimentation and agglomeration of fibres, samples were sonicated for 8 min before filtration. As regards solid samples, porous medium aliquots were resuspended in 10 mL deionized water and sonicated for 8 min to ensure

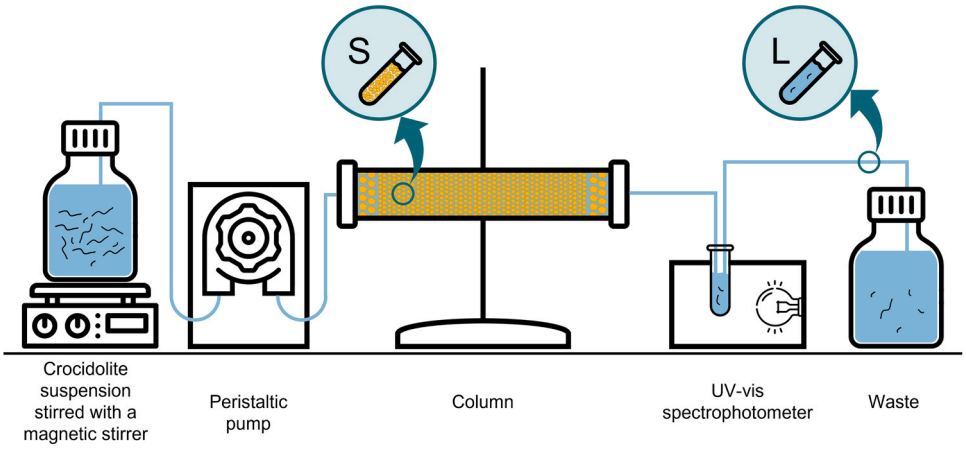

Fig. 1. Schematic rapresentation of the experimental setup used for crocidolite transport test; S and L represent, respectively, the solid and liquid sample location.

the complete detachment of crocidolite from the sand fraction. A 0.1 mL aliquot of the supernatant was then filtered on polycarbonate membranes with the same procedure applied for liquid samples. All the filtering membranes were left to dry at room temperature, adequately covered to avoid any contaminations. Then, membranes were mounted on aluminium sample holders using graphite tape and coated by a conductive graphite layer.

All liquid and solid samples membranes were analysed by means of a JEOL JSM IT300LV SEM with W emitter, coupled with an EDS Oxford INCA Energy 200 X-act SDD thin window detector. 0.1 mm^2 of each membrane surface was scanned acquiring 0.003 mm^2 images with a resolution of 32 pixel/μm.

For liquid samples, crocidolite was counted regardless of length, width, or aspect ratio after verifying the chemical composition. Concentration in f/L (F) was then calculated considering the volume of sample filtered through the porous membrane. In addition to the fibre number, the SEM image analysis allowed to measure the length and width of the fibres and to estimate their volume and mass by approximating their shape to a cylinder and considering a crocidolite density of 3.37 g/cm^3 [45]. The conversion of number concentration (f/L) into mass concentration (mg/L) was performed adapting an Italian guideline for massive samples investigations [12].

The quantitative analysis of liquid samples was performed only during the injection step (phase ii in Section 2.3). A qualitative analysis was instead performed on the liquid samples collected during the release step (phase iv in Section 2.3) to gain insights on the dimensional and morphological characteristics of the crocidolite released as a result of the pH variation of the flushing solution. As far as concern the "S" samples, SEM-EDS analyses were performed to obtain the morphological characteristics of crocidolite retained in the first segments of the column.

Throughout the paper "F" will be used to refer to crocidolite concentration in number (f/L) measured by SEM-EDS, while "M" to crocidolite concentration in mass (mg/L). "F5″ indicates the number concentration of fibres with AR $>$ 3, width $<$ 3 μm and length $>$ 5 μm, "F10″ indicates the number concentration of fibres with AR $>$ 3, width $<$ 3 μm and length $\geq$ 10 μm. Subscript "0" is added when the concentration refers to the injected suspensions.

3. Results and discussion

3.1. Characterisation of asbestos suspensions

The first batch, HC, shown in Fig. 2, was obtained by collecting the supernatant of the 300 mg/L crocidolite suspension after a 5 h settling. The suspension had an average concentration in number of $2.9{\cdot}10^{11}$ f/L

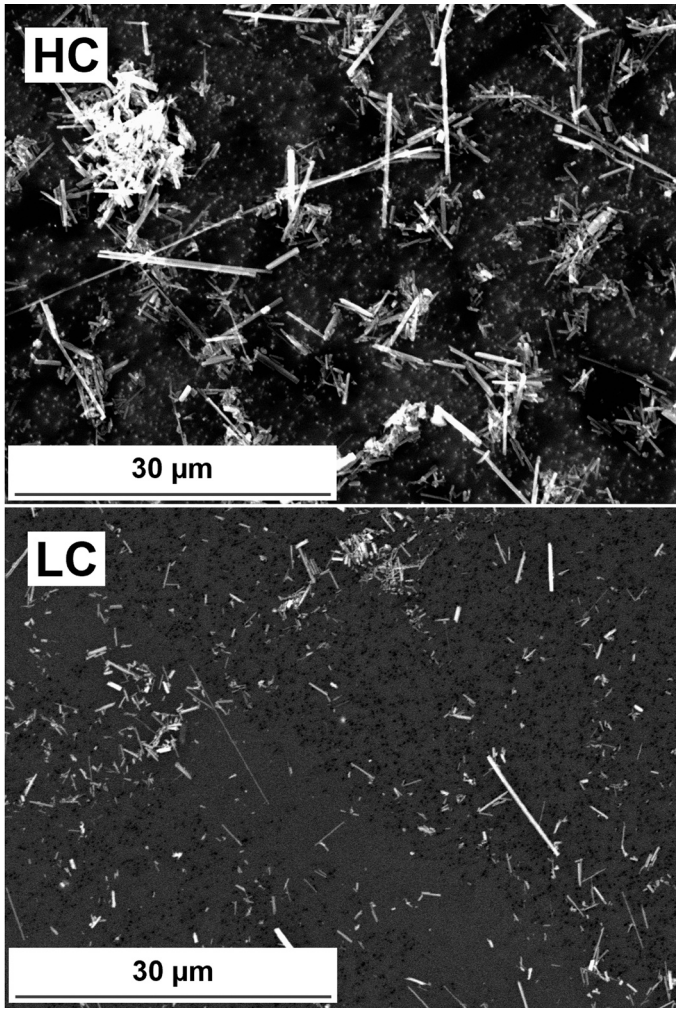

Fig. 2. SEM pictures of tested crocidolite suspensions. HC) high concentration suspension; LC) low concentration suspension.

(as shown in Table 1), which was evaluated by analysis of SEM images. The corresponding mass concentration of 92.9 mg/L was estimated as described in Section 2.4. The mean value of F5 was $1.6{\cdot}10^{10}$ f/L (5.5% of the total) and the mean value of F10 was $2.8{\cdot}10^{9}$ f/L (1.0% of the total). The maximum AR value was 102, while the average value was 10. The HC size distributions are shown in Fig. S6 (SI).

Table 1
F (f/L) and M (mg/L) concentrations of crocidolite in the inlet (HC) and in liquid samples collected at the column outlet (L1, L2, L3) during transport tests performed with the high concentration suspension (HC). F5, number concentration of fibres longer than 5 μm, and F10, number concentration of fibres longer than 10 μm values, are also reported. Dimension ranges (L=length, W=width) of detected fibres are reported for each sample. Additional details regarding quantitative results obtained on SEM-EDS analyses are reported in Table S3 (SI).

		F (f/L)	F5 (f/L)	F10 (f/L)	M (mg/L)	L_{min} (μm)	L_{max} (μm)	W_{min} (μm)	W_{max} (μm)
HC		$2.9{\cdot}10^{11}$	$1.6{\cdot}10^{10}$	$2.8{\cdot}10^{9}$	92.91	0.520	17.790	0.077	0.766
Coarse sand	L1	$6.3{\cdot}10^{10}$	$5.3{\cdot}10^{8}$	$1.1{\cdot}10^{8}$	3.81	0.292	18.138	0.044	0.554
	L2	$5.7{\cdot}10^{10}$	$1.1{\cdot}10^{8}$	-	3.69	0.311	6.205	0.062	0.560
	L3	$3.7{\cdot}10^{9}$	$5.3{\cdot}10^{7}$	-	0.56	0.330	7.343	0.083	0.466
Medium sand	L1	$6.3{\cdot}10^{9}$	$3.7{\cdot}10^{8}$	$1.1{\cdot}10^{8}$	2.25	0.517	18.248	0.069	0.532
	L2	$2.1{\cdot}10^{9}$	$7.0{\cdot}10^{7}$	-	0.22	0.436	6.151	0.056	0.348
	L3	$2.1{\cdot}10^{9}$	$2.1{\cdot}10^{7}$	-	0.22	0.404	6.468	0.075	0.405
Fine sand	L2	$7.8{\cdot}10^{8}$	$3.0{\cdot}10^{7}$	-	0.16	0.532	6.047	0.079	0.407
	L3	$8.9{\cdot}10^{8}$	$2.6{\cdot}10^{7}$	-	0.17	0.435	7.351	0.069	0.473

The second batch, LC, shown in Fig. 2, was obtained by filtering the HC suspension through a coarse sand bed using the setup described in Section 2.3. The resulting suspension had a concentration in number of $9.9{\cdot}10^{10}$ f/L, shown in Table 2, corresponding to a mass concentration of 5.5 mg/L, similar to the mass concentration detected in aquifers in NOA-rich areas [7]. The F5 concentration was $1.1{\cdot}10^{9}$ f/L (1.1% of the total) and the F10 concentration was $2.1{\cdot}10^{8}$ f/L (0.2% of the total). The AR mean value was 8 with a maximum of 92. The LC size distributions are shown in Fig. S6 (SI).

It must be noted that, despite the number concentration of fibres in the HC suspension is comparable to LC one ($2.9{\cdot}10^{11}$ f/L for the HC and $9.9{\cdot}10^{10}$ f/L for the LC), a substantial mass concentration difference between the two suspensions is observed (92.9 mg/L for the HC and 5.5 mg/L of the LC). This discrepancy between the number and mass concentration is justified by the different fibre size distribution in the two samples. In particular, the F5 value is higher in the HC suspension than in the LC one. These fibres contribute significantly to the total asbestos mass in the samples; indeed, the F5 amount is one order of magnitude higher in the HC suspension ($1.6{\cdot}10^{10}$ f/L) than in the LC one ($1.1{\cdot}10^{9}$ f/L). On the contrary, the LC suspension contains a high number of shorter fibres, which do not contribute significantly to the total asbestos mass in the samples.

3.2. Column transport tests

Two sets of transport tests, conducted by injecting crocidolite suspensions in 1D columns filled with sand material, were performed to probe the mobility of the fibres mimicking two realistic scenarios. The first set was conducted to simulate the mobility of a highly concentrated suspension (HC) in an aquifer system close to the source of contamination, the second to investigate the transport of a low concentrated suspension (LC) in a contaminated plume far from the release zone. The following sections describe the influence of asbestos size and concentration, and of the porous media granulometry, and of physicochemical parameters on the crocidolite mobility.

3.2.1. HC transport experiments

The first set of column tests was performed injecting the HC suspension through three types of quartz sand with different grain size distributions (coarse, medium and fine). The breakthrough curve (Fig. 3) of the experiment in coarse sand showed C/C_0 values greater than 20% during the whole injection step, with a maximum value of 30% observed at about 2 PV. Lower values, namely 2.2% and 0.3%, were respectively found for the medium and fine sand after 3 PV from the start of the injection. A higher retention of the crocidolite is observed when reducing the grain size distribution of the sand. This trend is also confirmed by the number concentration determined by SEM-EDS analyses (Table 1), which shows F values for the coarse, medium and fine sand equal to $5.7{\cdot}10^{10}$ f/L, $2.1{\cdot}10^{9}$ f/L, and $7.8{\cdot}10^{8}$ f/L respectively, for the liquid samples L2 collected after 3 PV at the outlet of the column. The corresponding M values, 3.69 mg/L for coarse, 0.22 mg/L for medium and 0.16 mg/L for fine sand, reflect the same tendency (Table 1). These results indicate that, despite a large amount of the injected asbestos is filtered out by the sandy media, a non-negligible fraction of the fibres is still mobile.

These results prove that crocidolite with a negatively charged surface can be transported, even in the absence of DOM, through negatively charged quartz sands. However, since only fibres longer than 5 μm (characterized by width < 3 μm and AR > 3) are considered dangerous to health if respired [50], it is of crucial importance to also assess the geometric characteristics of the fibres. As reported in Table 1, the average concentration of fibres longer than 5 μm ($F5_0$) in the injected HC suspension was equal to $1.6{\cdot}10^{10}$ f/L, the 17.5% of which consisted in fibres even longer than 10 μm ($F10_0$ equal to $2.8{\cdot}10^{9}$ f/L). All the

Table 2
F (f/L) and M (mg/L) concentrations of crocidolite in the inlet (LC) and in liquid samples collected at the column outlet (L1, L2, L3) during transport tests performed with the low concentration suspension (LC). F5, number concentration of fibres longer than 5 μm, and F10, number concentration of fibres longer than 10 μm values, are also reported. Dimension ranges (L=length, W=width) of detected fibres are reported for each sample. Additional details regarding quantitative results obtained on SEM-EDS analyses are reported in Table S4 (SI).

		F (f/L)	F5 (f/L)	F10 (f/L)	M (mg/L)	L_{min} (μm)	L_{max} (μm)	W_{min} (μm)	W_{max} (μm)
LC		$9.9{\cdot}10^{10}$	$1.1{\cdot}10^{9}$	$2.1{\cdot}10^{8}$	5.49	0.191	13.223	0.049	0.404
Coarse sand	L1	$4.3{\cdot}10^{9}$	$1.1{\cdot}10^{8}$	$2.1{\cdot}10^{7}$	1.14	0.435	11.830	0.104	0.528
	L2	$5.8{\cdot}10^{9}$	$2.1{\cdot}10^{7}$	-	0.93	0.354	5.044	0.070	0.551
	L3	$6.5{\cdot}10^{9}$	$1.5{\cdot}10^{8}$	$2.1{\cdot}10^{7}$	1.18	0.317	14.530	0.070	0.762
Medium sand	L1	$5.4{\cdot}10^{9}$	$4.2{\cdot}10^{7}$	-	0.43	0.243	8.821	0.070	0.379
	L2	$3.8{\cdot}10^{9}$	$6.3{\cdot}10^{7}$	-	0.39	0.267	9.189	0.066	0.423
	L3	$2.3{\cdot}10^{9}$	$4.2{\cdot}10^{7}$	-	0.28	0.386	6.683	0.088	0.325
Fine sand	L1	$3.7{\cdot}10^{9}$	$2.1{\cdot}10^{7}$	-	0.75	0.311	5.144	0.062	0.543
	L2	$2.8{\cdot}10^{9}$	$1.1{\cdot}10^{7}$	-	0.38	0.352	5.256	0.063	0.517
	L3	$1.7{\cdot}10^{9}$	$1.1{\cdot}10^{7}$	-	0.19	0.320	5.532	0.072	0.418

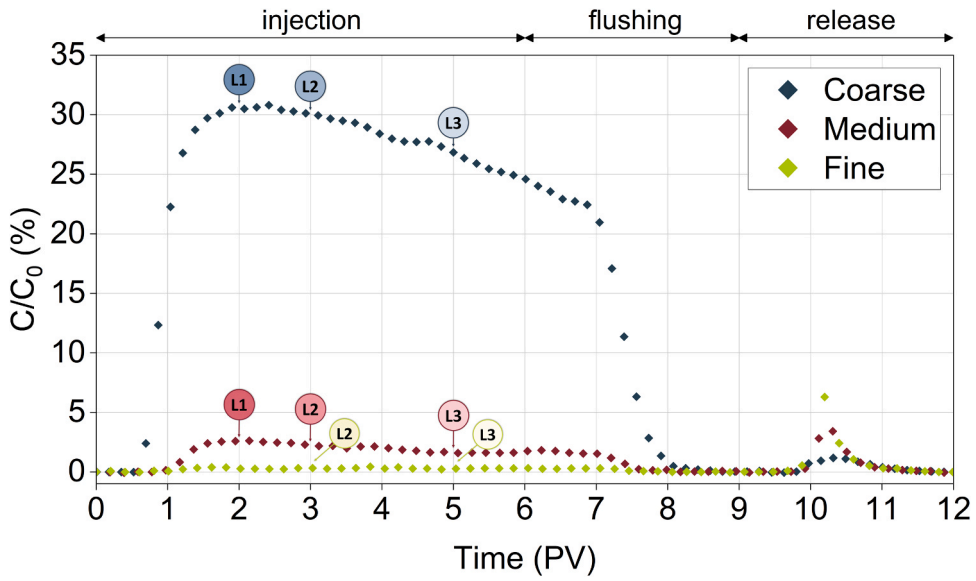

Fig. 3. Experimental breakthrough curves of normalized absorbance concentration of HC crocidolite suspension during transport experiments performed in quartz sand with different granulometry (coarse, medium, fine). Labels correspond to the liquid samples (L) collected at the column outlet and analysed by SEM-EDS.

outlet samples are characterized by a F5 count well above 10^7 f/L and more specifically in the range $2.1{\cdot}10^7$-$5.3{\cdot}10^8$ f/L (Table 1). The concentrations of these samples are comparable or higher than the ones found in suspensions used by Avataneo et al. (2022) [4] and by Roccaro and Vagliasindi (2018) [38], who reported that waterborne values of $4.4{\cdot}10^7$ f/L and in the range $7.9{\cdot}10^3$-$2.5{\cdot}10^4$ f/L, respectively, can cause an airborne contamination above the 1 f/L attention threshold [49], whether the water-to-air migration of fibres is triggered under specific conditions.

Fibres up to 18 μm were found in outlet samples of coarse and medium sand tests (see L_{max} in Table 1), while fibres up to 7 μm were measured in the fine sand test outlet. In particular, the 0.8% (coarse), 0.5% (medium) and 0.2% (fine) of $F5_0$ were recovered at the column outlet after 3 PV of suspension injection (L2, Fig. 4). Conversely, fibres longer than 10 μm were found only in sample L1 at the outlet of the coarse and medium sand columns. In these two samples the same F10 concentration value was found, $1.1{\cdot}10^8$ f/L, which is higher than the EPA maximum contaminant level for drinking water ($7{\cdot}10^6$ f/L for fibres longer than 10 μm). The results of the column tests performed at HC highlight that fibres longer than 10 μm barely migrate, while crocidolite with length between 5 and 10 μm might be substantially transported through sandy aquifers.

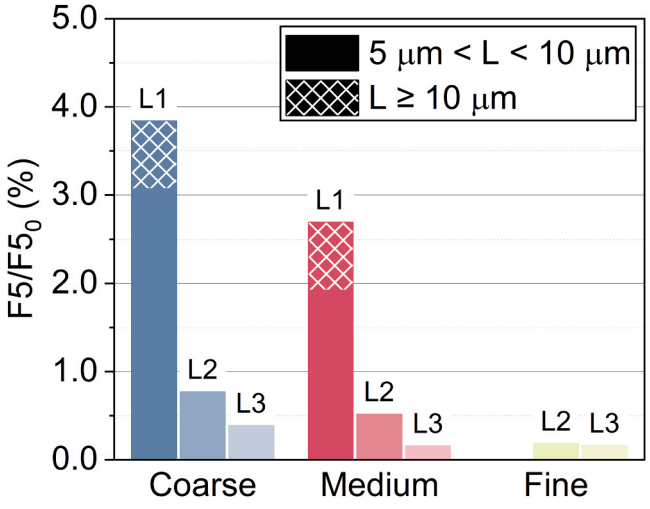

Fig. 4. Bar chart of concentration of fibres longer than 5 μm (F5) in liquid samples collected at the column outlet (L1, L2, L3) as a percentage of concentration of fibres longer than 5 μm of the HC suspension ($F5_0$) for the three tested sands (coarse, medium, fine); solid fill) the portion of fibres longer than 5 μm and shorter than 10 μm; pattern fill) the portion of fibres longer than (or equal to) 10 μm.

As far as concern transport mechanisms, the particle deposition in porous media is considered the result of both physical (i.e. thick particles trapped in small pores of the porous medium) and physicochemical processes (i.e. particle attachment on the porous medium surface due to attractive particle-grain interaction forces). The first mechanism is typically assumed irreversible, meaning that no particle remobilization is expected upon a change of the pore water chemistry. As for attachment, instead, a variation of hydrochemical conditions (e.g. pH increase) may induce a detachment of the deposited particles due to the reduction of the attractive forces between the particles and the sand grains.

In the case of crocidolite, physical filtration in small pores is expected to play a major role for the longer fibres. The fibre physical filtration can be a combination of several mechanisms such as mechanical filtration (when particles are larger than or about the same size of small pores, [13]), straining (particles are trapped in the down-gradient pore throats that are too small to allow the particle passage, [6]), and hydrodynamic bridging (when several particles simultaneously arrive at the inlet of a pore throat and form a colloid bridge, [25,26]). All three physical mechanisms presented are function of the relationship between particle size and pore throat dimension and they increase when decreasing the pore size maintaining constant the inlet suspension. This is in agreement with the higher retention of the crocidolite observed when reducing the sand grain size distribution. However, due to the peculiar shape of asbestos and to the heterogenous size of the fibres considered in this study, it is very difficult to predict which of these mechanisms would prevail. These mechanisms result in an exponential or hyper-exponential retention profile. Indeed, the SEM-EDS analysis of porous media samples (HC_S1_Coarse, HC_S1_Medium, HC_S1_Fine) collected at the first column centimetre for each tested sand (coarse, medium, and fine) presented a high number of fibres longer than 5 μm and even longer than 10 μm (Fig. 5). Moreover, visual inspection confirmed that the length of trapped fibres increases when decreasing the sand grain size distribution.

Another evidence confirming the occurrence of physical filtration

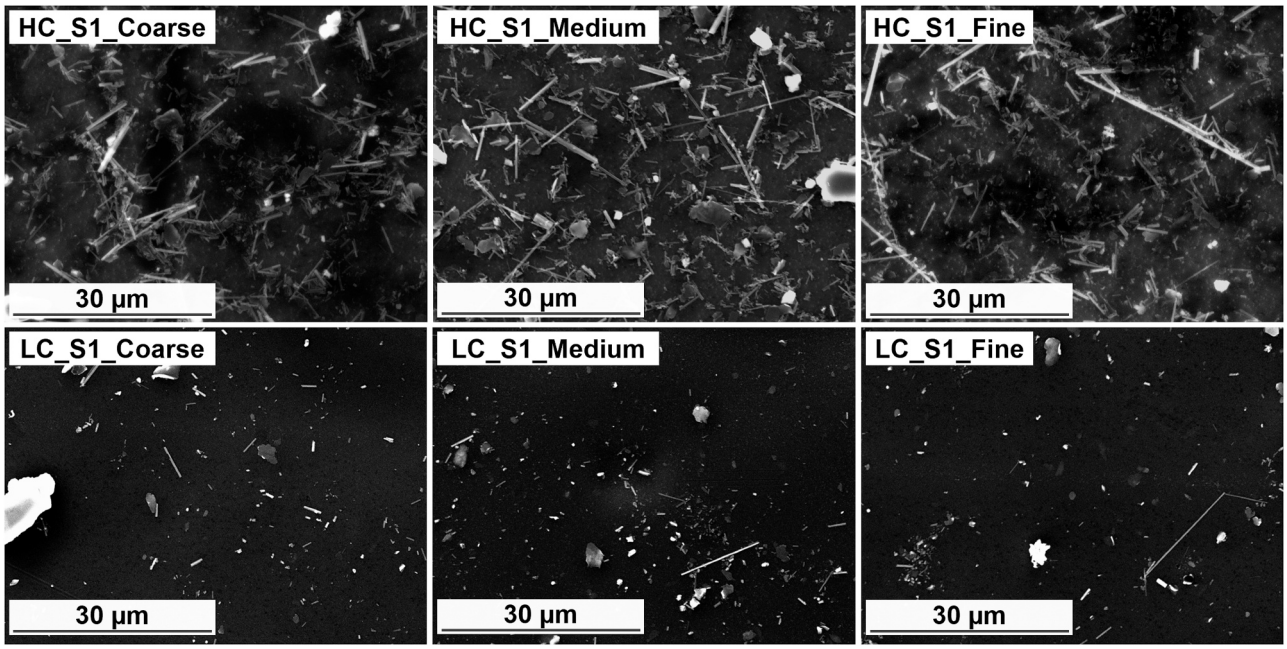

Fig. 5. SEM pictures of the porous media samples collected from the first column centimetre after the transport test with: HC suspension for coarse sand (HC_S1_Coarse), medium sand (HC_S1_Medium), fine sand (HC_L1_Fine); LC suspension for coarse sand (LC_S1_Coarse), medium sand (LC_S1_Medium), fine sand (LC_S1_Fine).

mechanisms is related to the evolution of the outlet concentration, which decreases over time once the filtered fibres start to clog the pores. This can be observed by the breakthrough curves reported in Fig. 3 where the absorbance ratio decreases from 30% to 22% for the coarse sand and from 2.5% to 1.5% for the medium sand. However, the decrease in absorbance is not evident for the fine sand, probably due to the low absorbance value detected. The increased filtration efficiency over time is also confirmed by the SEM-EDS analysis of the liquid samples collected at the column outlet, shown in Fig. 4. The graph shows a clear decrease over time (from sample L1 to sample L3) of the F5 values for all three quartz sands. In particular, the $F5/F5_0$ ratio decreases from 3.8% to 0.4% in coarse sand, from 2.7% to 0.2% in the medium sand, and from 0.18% to 0.16% in the fine one.

The release of reversibly attached fibres was induced by increasing the pH of the flushing water as this eliminates the energy barrier to detachment and creates repulsive forces that exist across all separation distances [36,42,5]. As shown by the BCs in Fig. 3, a significant release peak is observed during the NaOH flushing for all three sand types. The peak height is inversely proportional to the sand grain size distribution, suggesting that physicochemical processes are more intense in the finer sand than in the coarser one due to the greater surface area of the porous medium in fine sand. The fibre amounts detached during the release phase are the 0.18%, 0.32% and 0.40% of the injected one respectively for coarse, medium, and fine sand (Table S2, SI). This result suggests that the transport of the HC suspension is mainly influenced by physical retention mechanism, whereas attachment processes are playing a secondary role. A liquid sample was also collected during the release phase of the coarse sand column experiment and a SEM picture was acquired (Fig. S7, SI). The image demonstrates the presence of fibres in the eluate, some of them with length of about 5 µm. This result indicates that, even if initially retained by the porous medium, fibres may be remobilized if there is a change in the aquifer hydrochemical conditions. It should be noted that a high pH variation was induced during the release phase to estimate the total fraction of remobilized fibres. Consequently, the expected remobilized fibres in an aquifer system should be a portion of the total fraction.

3.2.2. LC transport experiments

The second set of column tests was carried out injecting the LC suspension through the three porous media. The resulting normalized absorbance curves are shown in Fig. 6. Similarly to what observed for HC suspension, the BCs show an increase of the crocidolite retention when reducing the grain size distribution of the sand. However, overall, the crocidolite low concentrated suspension shows a much higher mobility than the one observed during the HC experiments. The mobility increase is particularly pronounced for tests performed in the medium and fine sand, where the maximum value of C/C_0 increases from 1.1% (HC) to 18.4% (LC) for medium sand and from 0.5% (HC) to 9.7% (LC) for fine sand. The higher mobility of the LC suspension is probably due to the lower $F5_0$ value compared to HC one, in terms of both absolute number ($1.1{\cdot}10^9$ f/L for LC and $1.6{\cdot}10^{10}$ f/L for HC) and percentage on total (1.1% for LC and 5.5% for HC). Indeed, a lower content of long fibres is expected to reduce the effects of mechanical filtration, straining, and hydrodynamic bridging [25,26]. Moreover, the lower $F5_0$ reduces the probability of porous medium clogging, which would have resulted in an increase of the filtration efficiency over time. This is confirmed by the shape of the BCs in Fig. 6 that, differently from what observed during the HC experiments, remain relatively constant during all the injection phases.

From the results of the SEM-EDS analysis, F5 values range between $1.1{\cdot}10^7$ and $1.5{\cdot}10^8$ f/L for the outlet liquid samples (Table 2), which are of the same order of magnitude as the HC tests. Interestingly, due to a lower porous media clogging, a F10 amount higher than the EPA threshold for drinking water was found in the L1 and L3 samples of the coarse sand (Table 2). Also, relatively long fibres were found in the L2 sample of the coarse sand test, showing a maximum length of 9.541 µm (Table 2). Looking at the normalized F5 value over time (Fig. 7) a net decreasing trend was not observed for the LC tests, in contrast with what observed for HC set in Fig. 4. This is a further evidence of a minor porous media clogging. Nonetheless, a general decrease in $F5/F5_0$ values is seen when reducing the grain size distribution of the sand, confirming the trend mentioned above based on BCs (Fig. 6).

As for the HC experiments, a high pH flushing was performed at the end of the test to discriminate between reversible and irreversible fibre deposition. Despite the smaller amount of fibre retained in the column

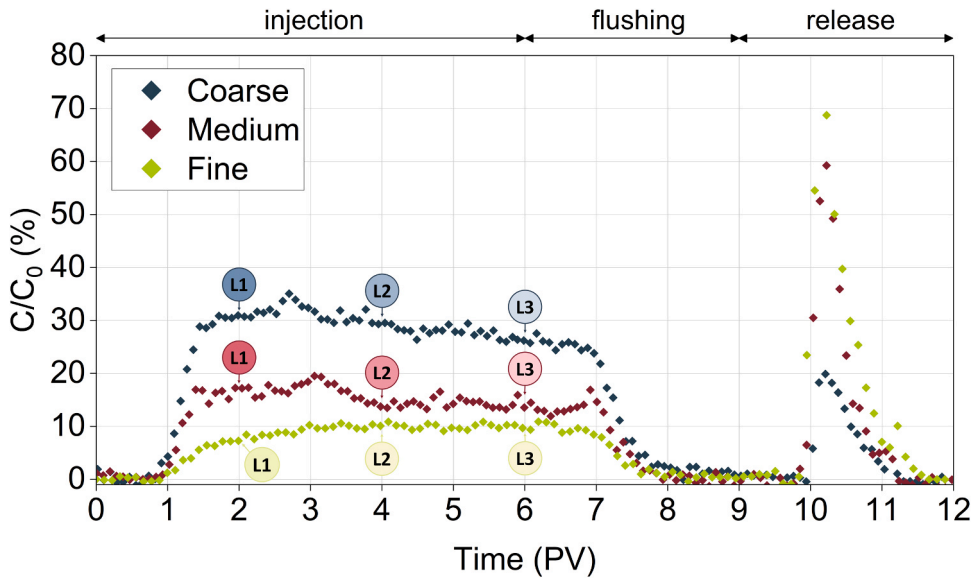

Fig. 6. Experimental breakthrough curves of normalized absorbance concentration of LC crocidolite suspension during transport experiments performed in quartz sand with different granulometry (coarse, medium, fine). Labels correspond to the liquid samples (L) collected at the column outlet and analysed by SEM-EDS.

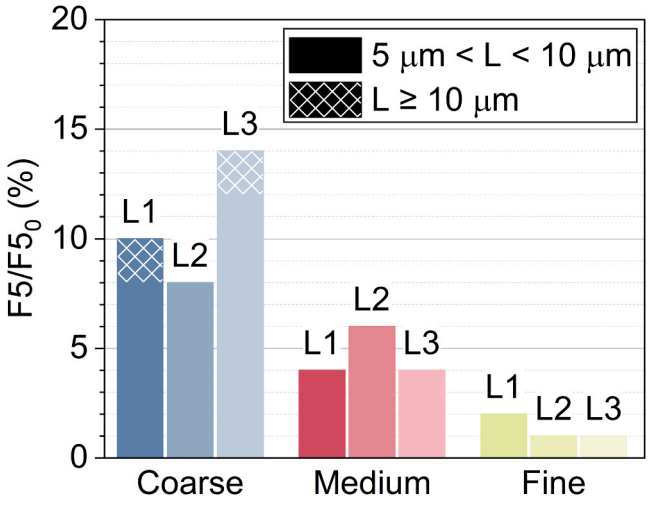

Fig. 7. Bar chart of concentration of fibres longer than 5 μm (F5) in liquid samples collected at the column outlet (L1, L2, L3) as a percentage of concentration of fibres longer than 5 μm of the LC suspension ($F5_0$) for the three tested sands (coarse, medium, fine); solid fill) the portion of fibres longer than 5 μm and shorter than 10 μm; pattern fill) the portion of fibres longer than (or equal to) 10 μm.

during the injection phase (i.e. higher BCs), the release peaks for the LC set result to be higher than for the HC tests. The release peak height varies from 18.0% to 68.8% for the tests performed with the LC suspension and from 1.2% to 6.3% for the HC one. The percentage of released fibres compared to injected fibres ranges between 1.95% and 7.00% for the LC column tests while from 0.18% to 0.40% for the HC column tests (Table S2, SI). This result indicates that physicochemical deposition processes are more relevant in the transport of the LC, while physical mechanism clearly prevails in the case of the HC suspension. This is in agreement with the larger size and higher concentration of fibres in the HC suspension, which result in a higher probability for particle retention due to mechanical filtration, straining and hydrodynamic bridging. This result suggests that asbestos transport may be influenced not only by physical filtration mechanisms, but also by physicochemical reversible processes.

The SEM images of the porous media portions sampled from the first centimetre of each column (LC_S1_Coarse, LC_S1_Medium, LC_S1_Fine in Fig. 5) revealed the presence of fibres in all the samples. More specifically, they showed the presence of fibres longer than 5 μm and 10 μm, but in a smaller amount compared to the HC samples. This is further evidence that clogging is lower for LC suspension compared to HC, due to the lower number of fibres longer than 5 μm trapped in the sand. Moreover, being reversible processes higher for LC suspension, most of the shorter fibres were flushed during the NaOH release phase and therefore are not visible in Fig. 5. The SEM pictures of the liquid samples collected during the release phase (Fig. S8, SI) show the presence of crocidolite with length up to 5 μm, particularly in medium and fine sand tests.

4. Conclusion

This study investigated the transport mechanism of waterborne crocidolite in saturated porous media mimicking sandy aquifers. Crocidolite was selected to represent amphibole asbestos behaviour, which exhibits negative net surface charge in water at any pH. Although asbestos mobility in subsoil has been generally neglected (or considered negligible), the results here presented show that bare crocidolite can be mobile in negatively charged porous media such as quartz sand aquifers.

Our results show that highly concentrated crocidolite suspensions generally determine lower breakthrough concentrations at the outlet of the columns due to the clogging of the porous medium which is induced mainly by physical filtration mechanisms (mechanical filtration, straining, or hydrodynamic bridging). The decrease of the grain size distribution of the porous medium determines a strong decrease of the output concentrations further confirming the important role of physical filtration mechanisms. On the contrary the injection of low concentration suspensions corresponds to a higher fibre recovery (if normalized to inlet concentration). Under these conditions, the decrease of the grain size of the porous media determines a less pronounced decrease in outlet concentrations. The transport is thus less influenced by the physical filtration mechanisms (due to the reduced number of long fibres) but it is still dependent on the physicochemical interactions occurring under unfavourable deposition conditions (since the fibres and collectors are characterized by the same surface charge).

By characterising the fibre suspensions sampled from the column outlet, we demonstrated that the medium and fine sandy media can

retain most of the fibres longer than 10 μm, while 5-to-10-μm-long fibres (which are still considered respirable by the WHO), can easily flow through. These results, obtained under specific laboratory conditions, might suggest that precautions should be taken to avoid water vaporisation or air dispersion of fibres in the case of groundwater extracted downstream from a contamination source.

Results obtained also indicate that fibres longer than 10 μm could migrate downwards a source of contamination in coarser aquifer systems and pose a hazard in the case of water-to-air migration of fibres, as for 5-to-10-μm-long fibres. Although water containing long fibres (length $>$ 10 μm) would be considered potentially safe to drink according to currently known scientific data for fibre ingestion, we believe that further investigations are necessary to ensure that no noxious effects could derive after direct oral intake. Indeed, fibres longer than 10 μm must be taken into account according to the guidelines expressed by the US-EPA with reference to the maximum contaminant level of asbestos in drinking water, established as a precautionary measure based on in vivo studies.

In addition, our results indicate that a change in the water physicochemical parameters, e.g. a pH increase, can remobilize fibres primarily attached to the porous media, proving that waters considered safe to use can become potentially harmful after natural or human induced events that cause alterations of the groundwater geochemistry.

This study provides evidence that groundwater migration serves as a potential pathway for exposure, emphasizing its inclusion in human health risk assessment evaluations. However, to enhance our understanding, it is imperative to conduct further research that focuses on elucidating the transport mechanisms governing asbestos migration over longer distances and time scales. This will enable a more accurate prediction of the decrease in fibre concentration as a function of the distance from the pollution source. Additionally, performing quantitative modelling of the experimental results will be a crucial step in assessing the potential risks posed to human health and the environment due to exposure to asbestos-contaminated drinking water.

CRediT authorship contribution statement

Leonardo Magherini: Conceptualization, Methodology, Investigation, Visualization, Writing – original draft, Writing – review and editing. **Chiara Avataneo**: Conceptualization, Methodology, Investigation, Visualization, Writing – original draft, Writing – review and editing. **Silvana Capella**: Visualization, Writing – review and editing. **Manuela Lasagna**: Visualization, Writing – review and editing. **Carlo Bianco**: Conceptualization, Investigation, Visualization, Writing – review and editing. **Elena Belluso**: Conceptualization, Funding acquisition, Supervision, Writing – review and editing. **Domenico Antonio De Luca**: Conceptualization, Funding acquisition, Supervision, Writing – review and editing. **Rajandrea Sethi**: Conceptualization, Funding acquisition, Supervision, Writing – review and editing.

Declaration of Competing Interest

The authors declare that they have no known competing financial interests or personal relationships that could have appeared to influence the work reported in this paper.

Data availability

Data will be made available on request.

Acknowledgements

The authors gratefully acknowledge the contribution of Dr. Sofia Credaro, who assisted in the language editing of the manuscript. Dr. Jasmine Rita Petriglieri is sincerely acknowledged for her support in laboratory activities.

Appendix A. Supporting information

Supplementary data associated with this article can be found in the online version at doi:10.1016/j.jhazmat.2023.131998.

References

[1] Al-Adeeb, A.M., Matti, M.A., 1984. Leaching corrosion of asbestos cement pipes. Int J Cem Compos Lightweight Concr. https://doi.org/10.1016/0262-5075(84)90018-6.
[2] ARPA - Agenzia Regionale per la Protezione Ambientale del Piemonte, 2021. Asbestos in water by Scanning Electron Microscopy (Amianto in acqua in Microscopia Elettronica a Scansione). U.RP.M842, rev.05.
[3] Avataneo, C., Belluso, E., Capella, S., Cocca, D., Lasagna, M., Pigozzi, G., et al., 2021. Groundwater asbestos pollution from naturally occurring asbestos (NOA): a preliminary study on the Lanzo valleys and Balangero plain area. NW Italy Ital J Eng Geol Environ 5–19. https://doi.org/10.4408/IJEGE.2021-01.S-01.
[4] Avataneo, C., Petriglieri, J.R., Capella, S., Tomatis, M., Luiso, M., Marangoni, G., et al., 2022. Chrysotile asbestos migration in air from contaminated water: An experimental simulation. J Hazard Mater. https://doi.org/10.1016/j.jhazmat.2021.127528.
[5] Beryani, A., Alavi Moghaddam, M.R., Tosco, T., Bianco, C., Hosseini, S.M., Kowsari, E., et al., 2020. Key factors affecting graphene oxide transport in saturated porous media. Sci Total Environ 698. https://doi.org/10.1016/j.scitotenv.2019.134224.
[6] Bradford, S.A., Yates, S.R., Bettahar, M., Simunek, J., 2002. Physical factors affecting the transport and fate of colloids in saturated porous media. Water Resour Res 38, 63–1-63–12. https://doi.org/10.1029/2002WR001340.
[7] Buzio, S., Pesando, G., Zuppi, G.M., 2000. Hydrogeological study on the presence of asbestos fibres in water of northern Italy. Water Res 34, 1817–1822. https://doi.org/10.1016/S0043-1354(99)00336-X.
[8] Chequer, L., Bedrikovetsky, P., Carageorgos, T., Badalyan, A., Gitis, V., 2019. Mobilization of attached clustered colloids in porous media. Water Resour Res 55, 5696–5714. https://doi.org/10.1029/2018WR024504.
[9] Cunningham, H.M., Pontefract, R., 1971. Asbestos fibres in beverages and drinking water. Nature 232, 332–333. https://doi.org/10.1038/232332a0.
[10] Di Ciaula, A., 2017. Asbestos ingestion and gastrointestinal cancer: a possible underestimated hazard. Expert Rev Gastroenterol Hepatol 11, 419–425. https://doi.org/10.1080/17474124.2017.1300528.
[11] Directive 2009/148/EC of the European Parliament and of the Council of 30 November 2009 on the protection of workers from the risks related to exposure to asbestos at work (Codified version) (Text with EEA relevance), 2009, OJ L.
[12] DM 06/06/1994. Regulations and technical methods relating to the cessation of the use of asbestos (Normative e metodologie tecniche di applicazione dell'art. 6, comma 3, e dell'art. 12, comma 2, della legge 27 marzo 1992, n. 257, relativa alla cessazione dell'impiego dell'amianto).
[13] Elimelech, M., 1995. Particle Deposition and Aggregation: Measurement, Modelling, and Simulation. Elsevier Science & Technology Books,.
[14] Fortunato, L., Rushton, L., 2015. Stomach cancer and occupational exposure to asbestos: A meta-analysis of occupational cohort studies. Br J Cancer 112, 1805–1815. https://doi.org/10.1038/bjc.2014.599.
[15] Granetto, M., Serpella, L., Fogliatto, S., Re, L., Bianco, C., Vidotto, F., et al., 2022. Natural clay and biopolymer-based nanopesticides to control the environmental spread of a soluble herbicide. Sci Total Environ 806, 151199. https://doi.org/10.1016/j.scitotenv.2021.151199.
[16] Gronow, J.R., 1986. Mechanisms of particle movement in porous media. Clay Miner 21, 753–767. https://doi.org/10.1180/claymin.1986.021.4.18.
[17] Hayward, S.B., 1984. Field monitoring of chrysotile asbestos in california waters. J AWWA 76, 66–73. https://doi.org/10.1002/j.1551-8833.1984.tb05301.x.
[18] Hu, Y., Hubble, D.W., 2007. Factors contributing to the failure of asbestos cement water mains. Can J Civ Eng 34, 608–621. https://doi.org/10.1139/l06-162.
[19] IARC Working Group on the Evaluation of Carcinogenic Risks to Humans, 2012. Arsenic, metals, fibres, and dusts. IARC Monogr Eval Carcinog Risks Hum 100, 11–465.
[20] IBAS - International Ban Asbestos Secretariat. Current Asbestos Bans. URL http://ibasecretariat.org/alpha_ban_list.php (last accessed 30/01/2023).
[21] INAIL - Istituto nazionale Assicurazione Infortuni sul Lavoro, 2022. Safe management of soils contaminated by asbestos of anthropic origin (Gestione in sicurezza di suoli contaminati da amianto di origine antropica).
[22] Kashansky, S.V., Slyshkina, T.V., 2002. Asbestos in water sources of the Bazhenovskoye chrysotile asbestos deposit. Int J Occup Med Environ Health 15, 65–68. ⟨https://pubmed.ncbi.nlm.nih.gov/12038867/⟩.
[23] Kohyama, N., Shinohara, Y., Suzuki, Y., 1996. Mineral phases and some reexamined characteristics of the International Union Against Cancer standard asbestos samples. Am J Ind Med 30, 515–528. https://doi.org/10.1002/(SICI)1097-0274(199611)30:5<515::AID-AJIM1>3.0.CO;2-S.
[24] Koumantakis, E., Kalliopi, A., Dimitrios, K., Gidarakos, E., 2009. Asbestos pollution in an inactive mine: Determination of asbestos fibers in the deposit tailings and water. J Hazard Mater 167, 1080–1088. https://doi.org/10.1016/j.jhazmat.2009.01.102.
[25] Lin, D., Hu, L., Alan Bradford, S., Zhang, X., Lo, I.M.C., 2022. Prediction of collector contact efficiency for colloid transport in porous media using Pore-Network and Neural-Network models. Sep Purif Technol 290, 120846. https://doi.org/10.1016/j.seppur.2022.120846.

[26] Lin, D., Hu, L., Bradford, S.A., Zhang, X., Lo, I.M.C., 2021. Pore-network modeling of colloid transport and retention considering surface deposition, hydrodynamic bridging, and straining. J Hydrol 603, 127020. https://doi.org/10.1016/j.jhydrol.2021.127020.
[27] Malinconico, S., Paglietti, F., Serranti, S., Bonifazi, G., Lonigro, I., 2022. Asbestos in soil and water: A review of analytical techniques and methods. J Hazard Mater 436, 129083. https://doi.org/10.1016/j.jhazmat.2022.129083.
[28] Mensi, C., Riboldi, L., De Matteis, S., Bertazzi, P.A., Consonni, D., 2015. Impact of an asbestos cement factory on mesothelioma incidence: global assessment of effects of occupational, familial, and environmental exposure. Environ Int 74, 191–199. https://doi.org/10.1016/j.envint.2014.10.016.
[29] Mohanty, S.K., Salamatipour, A., Willenbring, J.K., 2021. Mobility of asbestos fibers below ground is enhanced by dissolved organic matter from soil amendments. J Hazard Mater Lett 2, 100015. https://doi.org/10.1016/j.hazl.2021.100015.
[30] NTP - National Toxicology Program, 1985. NTP toxicology and carcinogenesis studies of chrysotile asbestos (CAS No. 12001-29-5) in F344/N Rats (Feed Studies). Natl Toxicol Program Tech Rep Ser 295, 1–390.
[31] Oliver, T., Murr, L. e, 1977. An electron microscope study of asbestiform fiber concentrations in rio grande valley water supplies. J AWWA 69, 428–431. https://doi.org/10.1002/j.1551-8833.1977.tb06784.x.
[32] OSHA - Occupational Safety and Health Standards, 2021. 29 CFR 1910.1001.
[33] Paglietti, F., Malinconico, S., Molfetta, V.D., Bellagamba, S., Damiani, F., Gennari, F., et al., 2012. Asbestos risk: from raw material to waste management: the italian experience. Crit Rev Environ Sci Technol 42, 1781–1861. https://doi.org/10.1080/10643389.2011.569875.
[34] Pelley, A.J., Tufenkji, N., 2008. Effect of particle size and natural organic matter on the migration of nano- and microscale latex particles in saturated porous media. J Colloid Interface Sci 321, 74–83. https://doi.org/10.1016/j.jcis.2008.01.046.
[35] Pollastri, S., Gualtieri, A.F., Gualtieri, M.L., Hanuskova, M., Cavallo, A., Gaudino, G., 2014. The zeta potential of mineral fibres. J Hazard Mater 276, 469–479. https://doi.org/10.1016/j.jhazmat.2014.05.060.
[36] Pulido-Reyes, G., Magherini, L., Bianco, C., Sethi, R., von Gunten, U., Kaegi, R., et al., 2022. Nanoplastics removal during drinking water treatment: Laboratory- and pilot-scale experiments and modeling. J Hazard Mater 436, 129011. https://doi.org/10.1016/j.jhazmat.2022.129011.
[37] Reid, A., Berry, G., de Klerk, N., Hansen, J., Heyworth, J., Ambrosini, G., et al., 2007. Age and sex differences in malignant mesothelioma after residential exposure to blue asbestos (Crocidolite) (Bill). Chest 131, 376–382. https://doi.org/10.1378/chest.06-1690.
[38] Roccaro, P., Vagliasindi, F.G.A., 2018. Indoor release of asbestiform fibers from naturally contaminated water and related health risk. Chemosphere. https://doi.org/10.1016/j.chemosphere.2018.03.040.
[39] Seymour, M.B., Chen, G., Su, C., Li, Y., 2013. Transport and retention of colloids in porous media: does shape really matter. Environ Sci Technol 47, 8391–8398. https://doi.org/10.1021/es4016124.
[40] Tian, Y., Gao, B., Wang, Y., Morales, V.L., Carpena, R.M., Huang, Q., et al., 2012. Deposition and transport of functionalized carbon nanotubes in water-saturated sand columns. J Hazard Mater 213–214, 265–272. https://doi.org/10.1016/j.jhazmat.2012.01.088.
[41] Ting, H.Z., Bedrikovetsky, P., Tian, Z.F., Carageorgos, T., 2021. Impact of shape on particle detachment in linear shear flows. Chem Eng Sci 241, 116658. https://doi.org/10.1016/j.ces.2021.116658.
[42] Tosco, T., Tiraferri, A., Sethi, R., 2009. Ionic strength dependent transport of microparticles in saturated porous media: modeling mobilization and immobilization phenomena under transient chemical conditions. Environ Sci Technol 43, 4425–4431. https://doi.org/10.1021/es900245d.
[43] Turci, F., Favero-Longo, S.E., Gazzano, C., Tomatis, M., Gentile-Garofalo, L., Bergamini, M., 2016. Assessment of asbestos exposure during a simulated agricultural activity in the proximity of the former asbestos mine of Balangero, Italy. J Hazard Mater 308, 321–327. https://doi.org/10.1016/j.jhazmat.2016.01.056.
[44] US-EPA - United States Environmental Protection Agency, 2021. 40 CFR 141.62.
[45] US-EPA - United States Environmental Protection Agency, 1983. Analytical method for determination of asbestos fibers in water.
[46] Wallis, S.L., Emmett, E.A., Hardy, R., Casper, B.B., Blanchon, D.J., Testa, J.R., et al., 2020. Challenging global waste management – bioremediation to detoxify asbestos. Front Environ Sci 8. https://doi.org/10.3389/fenvs.2020.00020.
[47] Wei, B., Ye, B., Yu, J., Jia, X., Zhang, B., Zhang, X., et al., 2013. Concentrations of asbestos fibers and metals in drinking water caused by natural crocidolite asbestos in the soil from a rural area. Environ Monit Assess 185, 3013–3022. https://doi.org/10.1007/s10661-012-2768-9.
[48] WHO - World Health Organization, 2021. Asbestos in drinking water: background document for development of WHO Guidelines for drinking-water quality. World Health Organization,.
[49] WHO - World Health Organization, 2000. Air quality guidelines for Europe. World Health Organization. Regional Office for Europe.
[50] WHO - World Health Organization, 1986. Asbestos and other natural mineral fibres. World Health Organization.
[51] Wu, L., Ortiz, C.P., Jerolmack, D.J., 2017. Aggregation of elongated colloids in water. Langmuir 33, 622–629. https://doi.org/10.1021/acs.langmuir.6b03962.